

# RSC Advances



This is an *Accepted Manuscript*, which has been through the Royal Society of Chemistry peer review process and has been accepted for publication.

*Accepted Manuscripts* are published online shortly after acceptance, before technical editing, formatting and proof reading. Using this free service, authors can make their results available to the community, in citable form, before we publish the edited article. This *Accepted Manuscript* will be replaced by the edited, formatted and paginated article as soon as this is available.

You can find more information about *Accepted Manuscripts* in the [Information for Authors](#).

Please note that technical editing may introduce minor changes to the text and/or graphics, which may alter content. The journal's standard [Terms & Conditions](#) and the [Ethical guidelines](#) still apply. In no event shall the Royal Society of Chemistry be held responsible for any errors or omissions in this *Accepted Manuscript* or any consequences arising from the use of any information it contains.

Cite this: DOI: 10.1039/c0xx00000x

www.rsc.org/xxxxxx

PAPER

# Controllable preparation of graphene oxide/metal nanoparticles hybrids as surface-enhanced Raman scattering substrates for 6-mercaptopurine detection

Wen Liang Fu<sup>a</sup>, Shu Jun Zhen<sup>\*a</sup>, Cheng Zhi Huang<sup>\*a,b</sup>

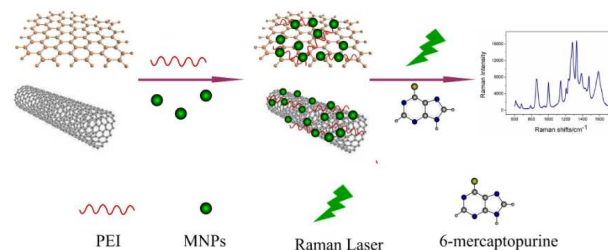
Received (in XXX, XXX) Xth XXXXXXXXX 20XX, Accepted Xth XXXXXXXXX 20XX  
DOI: 10.1039/b000000x

## Abstract

In this contribution, a new simple and cost-effective strategy for the preparation of the hybrids of graphene oxide (GO) and metal nanoparticles (MNPs) through the mediation of polyethyleneimine (PEI) molecules was reported. PEI molecules as cationic polymers could effectively attach on the surface of GO for further negative MNPs adsorption. By this process, gold and silver nanoparticles are assembled on GO with high efficiency. This method has also been successfully applied for the assembly of metal nanoparticles and carbon nanotubes (CNTs), indicating that this method is general. Furthermore, the as-prepared graphene oxide/ silver nanoparticles (GO/AgNPs) hybrids have been used as perfect surface enhanced Raman scattering (SERS) substrates with the enhancement factor at  $1.5 \times 10^5$  and successfully applied for the sensitive and selective detection of 6-mercaptopurine (6MP) in pharmaceutical tablets with satisfactory results.

## 1. Introduction

In recent years, famous carbon nanomaterials including graphene and carbon nanotubes have been popularly used as surface enhanced Raman scattering (SERS) substrates through chemical enhanced mechanism.<sup>1-4</sup> However, the deficiency is their relative weak Raman enhanced effect contrast with electromagnetic enhanced mechanism of noble metal nanomaterials, which restricts the analytical applications of carbon nanomaterials as SERS substrates. To address this issue, many researchers focus on assembling these famous carbon nanomaterials with metal nanoparticles (MNPs). For combined chemical and electromagnetic enhanced mechanism, these hybrids can be applied for SERS detection with high sensitivity. Moreover, functionalized carbon nanomaterials have the abilities of condensing molecules for further improving the sensitivity in SERS detection because of their large surface areas and unique electronic structures.<sup>5</sup> For example, Liu et al. successfully prepared graphene oxide and silver nanoparticles hybrids (GO/AgNPs) and used them in sensitive detection of trinitrotoluene.<sup>6</sup> Wang et al. and Huang et al. constructed GO or single walled carbon nanotubes (SWCNTs) with gold or silver nanoparticles assemblies for intracellular Raman mapping using the enhanced Raman signal of carbon nanomaterials.<sup>7,8</sup> Thus, to develop effective methods to prepare the carbon nanomaterials and MNPs hybrids are essential.



**Scheme 1** A scheme (not to scale) to illustrate the proposed preparation method of GO/MNPs hybrids and their application in the detection of 6-mercaptopurine.

Up to now, the wet chemical methods about construction of carbon nanomaterials and MNPs hybrids mainly include the way of in situ method and self-assembled method. By in situ method, the synthesis procedure is simple and no need to adding other linker molecules, but the morphology and density of MNPs is difficult to control. In contrast, self-assembly is an ordinary method to fabricate the carbon nanomaterials and MNPs hybrids because the loading ration and the morphology of the nanoparticles are tunable.<sup>5, 9</sup> However, most MNPs are synthesized with negatively charged reducing agents and capping agents, which makes them can not be anchored on negatively charged carbon nanomaterials directly. Therefore, various kinds of linker molecules, including protein,<sup>10</sup> DNA,<sup>11, 12</sup> and organic

small molecules<sup>13, 14</sup>, have been exploited to connect carbon nanomaterials and MNPs through different reactions, such as  $\pi$ - $\pi$  stacking, chemical bond formation and electrostatic adsorption.<sup>9, 11-13</sup> But most reported assembly strategies are complex for adding more operating steps. In addition, the linker molecules, such as protein and DNA, are expensive, and some linker molecules need to be synthesized through complex organic synthesis steps. Therefore, it is necessary to fabricate new assembly method, which is simple, cheap, and could be applied universally for the assemblies of other materials.

Herein, the GO and MNPs hybrids were fabricated by electrostatic self-assembly strategy. In our method, polyethyleneimine (PEI) molecules were served as linkers to prepare the stable cationic polyelectrolyte-functionalized GO for further MNPs anchoring (Scheme 1). PEI is a cationic polymer, which contains high density of amino groups. It has been proved that PEI has good affinity with GO through the electrostatic interaction,<sup>15, 16</sup> which makes the charge of GO reverse and easy to attach negatively charged MNPs. PEI is commercially available without the need to be synthesized, which make the process simple and easy to operate. In addition, it has been certified that this method is quite facile and MNPs can be attached on GO with high density. More importantly, this method was suitable for assembling MNPs on single walled carbon nanotubes (SWCNTs) and multi-walled carbon nanotubes (MWCNTs), confirming the good versatility of this method. The synthesized graphene oxide and silver nanoparticles hybrids (GO/AgNPs) could be used as efficient SERS substrates, which has been successfully applied for sensitive and selective detection of the chemotherapy drug 6-mercaptopurine (6MP) in tablets.

## 2. Experimental

### 2.1 Chemicals and Materials

All the chemicals were of analytical grade and used without further purification. Deionized distilled water (DI water) was used throughout. 6-Mercaptopurine, as standard sample, was purchased from National Institutes for Food and Drug Control. 6-Mercaptopurine tablets were purchased from Zhebei Pharmaceutical Co. Ltd. (Zhejiang, China). GO was supplied by the XF Nano, INC. (Shanghai, China). Single-walled carbon nanotubes (SWNTs) were supplied by Sigma and multi-walled carbon nanotubes (MWNTs) were supplied by Chengdu Organic Reagent Co. Ltd. (Chengdu, China). Polyethyleneimine (PEI) at molecular weight of 1.8 K was purchased from Aladdin. Other reagents include Hydrogen tetrachloroaurate (III) tetrahydrate (HAuCl<sub>4</sub>·4H<sub>2</sub>O), silver nitrite (AgNO<sub>3</sub>), and reagents for selectivity experiments are commercially available. Britton-Robinson (BR) buffer (pH 2.0) was employed for acidity control.

### 2.2 Characterization

Scanning electron microscopy (SEM) images were captured using an S-4800 scan electron microscopy (Hitachi, Japan). The absorption spectra were measured using a U-3010 UV-vis spectrophotometer (Hitachi, Japan). Transmission electron microscopy (TEM) images were captured using an S-4800 scan electron microscopy (Hitachi, Japan) equipped with a transmission accompaniment (HHTNT-539-9739, Hitachi). Zeta-

potential measurements were performed using a Zetasizer Nano-ZS90 instrument (Malvern Inc). Raman spectra were recorded using a LabRam HR 800 spectrometer (HORIBA Jobin Yvon, France).

### 2.3 Synthesis of GO and MNPs hybrids

For preparation of GO/PEI complex, PEI solution (100 mg mL<sup>-1</sup>) was slowly added to GO solution (1 mg mL<sup>-1</sup>) to make the weight ratio of GO: PEI is 2:1 under stirring. Then the mixture was ultrasonicated about 30 min, stirred overnight and washed 3 times with DI water by centrifugation and re-dispersed. For the procedure of assembling AgNPs or AuNPs to GO/PEI sheets, 25  $\mu$ L GO/PEI aqueous was added to 1 mL AgNPs or AuNPs solution for stand with several hours. The precipitate was washed several times and re-dispersed in 0.5 mL DI water.

The synthesis methods of 12 nm AgNPs and 13 nm AuNPs were referred to the reported methods.<sup>11</sup> For preparing of AgNPs, 1 mL 50 mM AgNO<sub>3</sub> and 1 mL 5% (w/w) sodium citrate was added to 48 mL DI water under vigorous string. Then a small amount of NaBH<sub>4</sub> solid was added to the mixture. Rapidly, the color of the solution was changed to brown-yellow, indicating the formation of AgNPs. The AgNPs aqueous was continuously stirred until the color keeps no change. Then, the AgNPs were centrifuged by 12 000 rpm for 15 min, the precipitate was removed and collected the supernatant for further use. For synthesis of AgNPs, 2 mL 1% (w/w) HAuCl<sub>4</sub>·4H<sub>2</sub>O solution was added to 48 mL of DI water under stirring. The mixture was then heated to boiling under stirring, and 1 mL 5% sodium citrate was added to the solution. Under continuous stirring and boiling, the mixture was gradually changed to wine red within 3 min. after boiling for another 20 min, the solution was cooled to room temperature under vigorous stirring.

### 2.4 Procedure for SERS detection

For the determination of 6MP, 30  $\mu$ L of the GO/AgNPs aqueous suspensions was mixed with 10  $\mu$ L 6MP dispersed in BR buffer (pH 2.0) with certain concentration. The mixture was allowed to stay for 1 hour to make the adsorption enough. Then, the samples in the solution phase were loaded in capillary tubes for SERS detection, with the laser beam focused on the center of a tube in both the longitude and transverse directions. Laser wavelength: 532 nm; power: 28 mW; lens: 10 $\times$  objective; acquisition time: 5s. For enhancement factor detection, laser wavelength: 532 nm; power: 2.45 mW; lens: 50 $\times$  objective; acquisition time: 5s.

### 2.5 6-Mercaptopurine tablets preparation

Ten tablets were weighed and ground into fine powder. 50 mg of powder was transferred into a 100 mL measuring flask and 50 mL 0.1 mol L<sup>-1</sup> HCl solution was added. The mixture was heated to be dissolved, then was cooled to room temperature. 0.1 mol L<sup>-1</sup> HCl was added to the mixture to the mark and filtrated. Appropriate amount of filtrate was diluted to 100 times for UV-vis absorption determination.

## 3. Results and discussion

### 3.1 Fabrication of carbon nanomaterials and MNPs hybrids

Branched PEI molecules with positive charges, which is generally used in small molecules or gene delivery and release,<sup>17-19</sup> can be directly adsorbed on the negatively charged carbon nanomaterials. In order to confirm the electrostatic assembly process occurred in solution, zeta-potential measurements were performed before and after GO adsorption with PEI and MNPs. Fig.1a showed that the average potential of pure GO solution was about -54.7 mV, indicating that a great deal of carboxyl groups and  $\pi$  electrons were scattered on the GO sheets. After assembled with PEI, the value was sharply increased to +42.1 mV, which confirmed the effective attachment occurred between GO and PEI. PEI functionalized GO with positive charge is a perfect building block for further decorating negatively charged MNPs. After adding AgNPs to GO/PEI mixture, the zeta-potential was decreased to -35.6 mV, indicating that AgNPs indeed assembled onto the surface of GO through the mediation of PEI. Fig.1b displayed the absorption spectra of GO/AgNPs and individual nanoparticles. Dispersive AgNPs have a characteristic absorption peak at 402 nm, and an 8 nm of red shift happened after forming GO/AgNPs, which attributed to the distance of AgNPs become smaller when dispersive AgNPs linked to GO sheets.<sup>12</sup> The intensity of absorption peak was reduced, also certifying the little aggregation of AgNPs occurred after AgNPs adsorption on GO surface.<sup>12, 20</sup>

The morphologies of GO/AgNPs were further characterized by TEM imaging as shown in Fig.1c&d. Although GO sheets were as thin as a wafer and mostly transparent, the area and edge of the AgNPs distributing let us believed that AgNPs indeed assembled on the GO surface. It was found there is deep color in some areas of GO/AgNPs, which was ascribed to the overlapping of loaded AgNPs. The results were also consistent with the red shift and reduction of absorption peak. In addition, AgNPs were attached on GO surface with high density, confirming that the GO/AgNPs hybrids were formed effectively. Similarly, gold nanoparticles (AuNPs) with negative charges could also connect with GO/PEI successfully. Fig.2a&b showed that the zeta-potential and absorption spectra have the similar tendency with AgNPs attach on GO/PEI. The TEM images of Fig.2c&d also confirmed the successful assembly between AuNPs and GO.

To further test the generality of the self-assembly strategy, other carbon nanomaterials including SWCNTs and MWCNTs were employed to assemble with MNPs. Carboxylated SWCNTs and MWCNTs with high negative charges played the similar role of GO and were easy to adsorb PEI molecules. As shown in Fig.3a&b, MWCNTs have the length about 0.4-2  $\mu\text{m}$  and the diameter is 10-50 nm. AuNPs and AgNPs engaged a compact layer around the MWCNTs, verifying the generality of the present assembly method. The result of SWCNTs/PEI react with metal nanoparticles was also shown in Fig.3c&d, further confirming the versatility and efficiency of present self-assembly strategy.

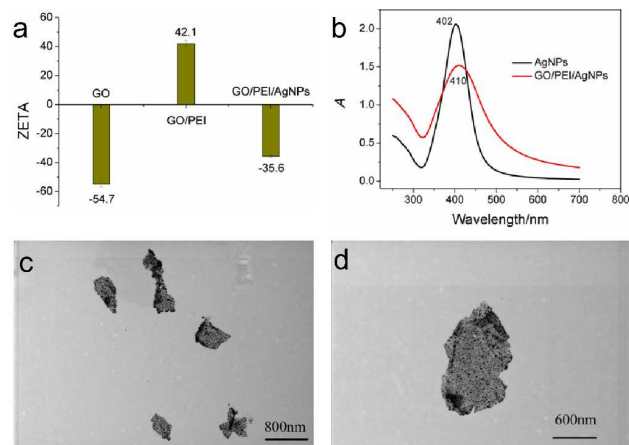


**Fig. 1** Zeta-potential measurements of GO, GO/PEI and GO/AgNPs hybrids in the aqueous solution (a); The UV-vis spectra of AgNPs and GO/AgNPs hybrids (b); TEM pictures of GO/AgNPs (c) and (d).

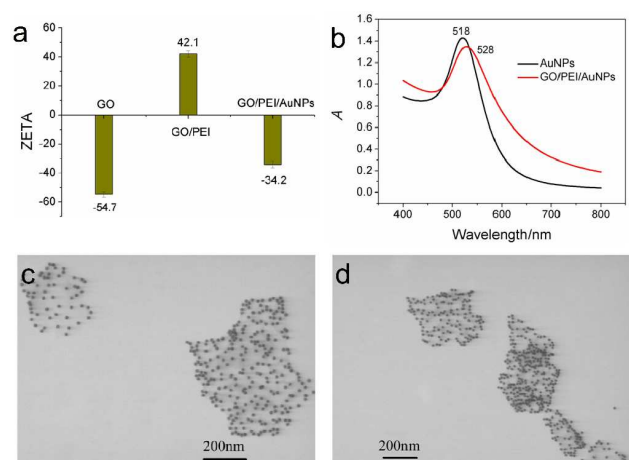


**Fig. 2** Zeta-potential measurements of GO, GO/PEI and GO/AuNPs hybrids in the aqueous solution (a); The UV-vis spectra of AuNPs and GO/AuNPs hybrids (b); TEM pictures of GO/AuNPs (c) and (d).

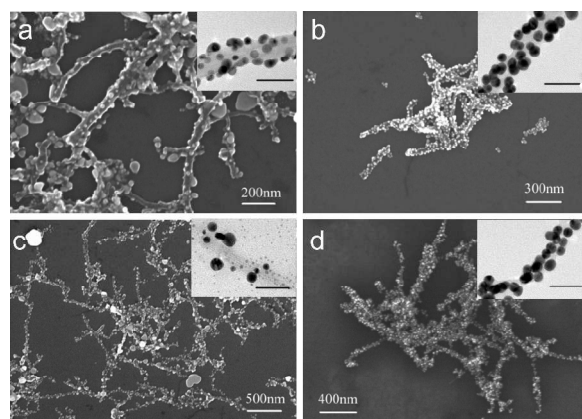


**Fig. 3** SEM pictures of MWCNT/AgNPs (a), MWCNT/AuNPs (b), SWCNT/AgNPs (c) and SWCNT/AuNPs (d). The insets show the TEM images of the hybrid materials with high magnification. The scale bar = 50 nm.

### 3.2 SERS property of the as-prepared GO/AgNPs hybrids

Because of the electromagnetic enhancement effect of AgNPs and AuNPs and chemical enhancement effect of carbon

nanomaterials, such nanocomposites can be potentially used as SERS substrates for sensitive analysis. To estimate the SERS activity of the carbon nanomaterials and MNPs hybrids, GO/AgNPs were chosen as typical substrates for enhancement factor (EF) calculating for the better enhancement effect of AgNPs than AuNPs.<sup>5</sup> 4-mercaptobenzoic acid (*p*MBA) was used as a model Raman probe because it has been well characterized by SERS in the range of 610-1800  $\text{cm}^{-1}$ . Fig.4 shows the characteristic Raman spectrum of solid *p*MBA and SERS spectrum of *p*MBA at  $5 \times 10^{-7}$  mol  $\text{L}^{-1}$  in the presence of GO/AgNPs substrate. According to previous studies, the predominant bands were located at 1084, 1188, and 1590  $\text{cm}^{-1}$ , which assigned to  $a_1$  modes of  $\nu\text{CS}$ ,  $\delta\text{CH}$ , and  $\nu\text{CC}$ .<sup>21, 22</sup> In the SERS spectrum, the  $\nu\text{CS}$  band at 1084  $\text{cm}^{-1}$  was shifted to 1079  $\text{cm}^{-1}$ , due to the Ag-S bond formation. The band  $\delta\text{CH}$  at 1188  $\text{cm}^{-1}$  was shifted to 1180  $\text{cm}^{-1}$ , and the  $\nu\text{CC}$  was shifted from 1590  $\text{cm}^{-1}$  to 1587  $\text{cm}^{-1}$  after *p*MBA adsorption on silver surface. To estimate the enhancement force of GO/AuNPs hybrids for *p*MBA, we calculated the SERS EF values using the following expression:<sup>23, 24</sup>

$$EF = (I_{SERS} N_{bulk}) / (I_{Raman} N_{surface}) \quad (1)$$

$I_{SERS}$  stands for the intensities of the vibrational mode of *p*MBA in the SERS spectra.  $I_{Raman}$  stands for the same vibrational mode with  $I_{SERS}$  in the normal Raman spectra of *p*MBA.  $N_{bulk}$  and  $N_{surface}$  are the number of *p*MBA molecules illuminated by the laser focus spot under normal Raman and SERS condition. All of these values can be obtained from the SERS spectra and Raman spectra.  $N_{surface}$  can be calculated according to the reported method.<sup>25</sup> Suppose the molecules were uniformly dispersed on the substrates, the density of *p*MBA on the film was assumed to be  $5 \times 10^{-7}$  mol  $\text{L}^{-1} \times 3 \mu\text{L} \times N_A / 7.0 \text{ mm}^2$  (the surface area of the substrate is  $7.0 \text{ mm}^2$ ), namely,  $1.3 \times 10^{11}$  molecules/ $\text{mm}^2$ .<sup>26</sup> The laser spot has a  $1 \mu\text{m}$  diameter and the surface area is about  $7.9 \times 10^{-7} \text{ mm}^2$ , so  $N_{surface}$  had a value of  $1.0 \times 10^5$ . Taking the laser spot ( $1 \mu\text{m}$  diameter), the penetration depth (about  $2 \mu\text{m}$ ), the density of the solid *p*MBA ( $1.06 \text{ g/cm}^3$ ) into account,<sup>27</sup>  $N_{bulk}$  had a value of  $6.6 \times 10^9$  in the detected solid sample area. All the spectra were normalized for laser power and acquisition time. The EF at the band at 1079  $\text{cm}^{-1}$  of *p*MBA can be calculated to be  $1.5 \times 10^5$  for the GO/AgNPs hybrids, and it is high enough to ultrasensitive analytical detection.

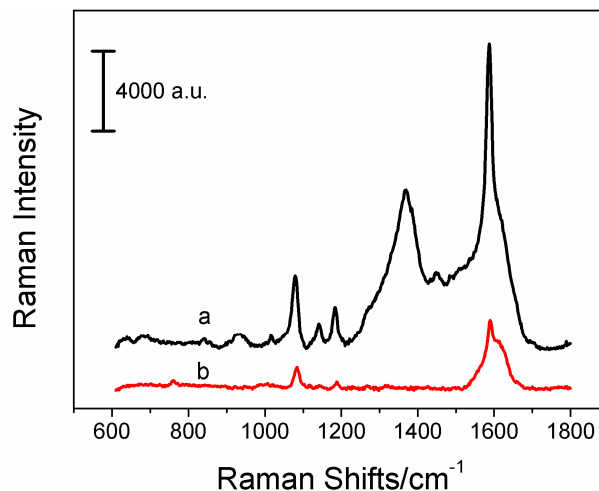
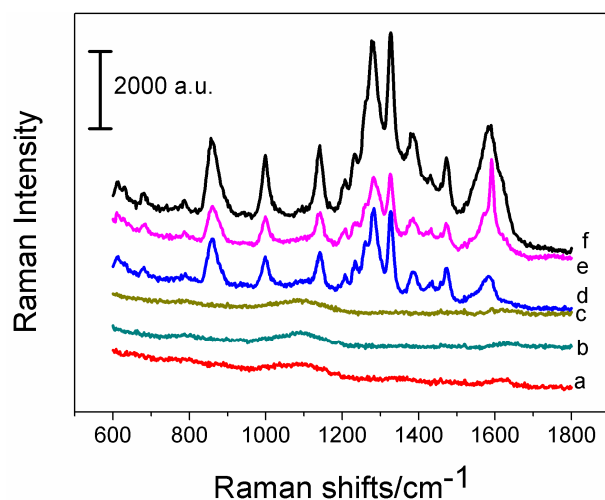


Fig. 4 SERS spectra of  $5 \times 10^{-7}$  mol  $\text{L}^{-1}$  *p*MBA on GO/AgNPs (a) and Raman spectra of solid *p*MBA (b).

### 3.3 GO/AgNPs as SERS substrate for 6MP detection

As a chemotherapy drug, 6MP employed in the treatment of a variety of diseases for many years, including rheumatologic disorders, immunodiseases, post-transplant immunosuppression, inflammatory bowel diseases, and lymphoblastic leukemia.<sup>28</sup> However, some adverse effects produced after taking more 6MP, including myelosuppression and bone-marrow suppression.<sup>29</sup> Therefore, 6MP detection is with biological significances. 6MP is a planar molecule that can attach on metal surface with possible binding site of N and S groups, and it has been proved that 6MP modified gold nanoparticles exhibited the enhanced drug delivery<sup>30</sup> and applied in biomedical filed.<sup>30, 31</sup> A previous work has shown that 6MP can be efficiently adsorbed on AgNPs and exhibited fairly strong SERS signals.<sup>32</sup> Therefore, we can construct a label free and sensitive SERS method for determination of 6MP by using the assemblies of carbon nanomaterials and metal nanoparticles as substrates.

As shown in Fig.5, a series of SERS spectra of  $5 \mu\text{mol L}^{-1}$  6MP on different substrates were achieved. It was found that, in the liquid condition, the signal of 6MP could be present just with carbon nanomaterials and silver nanoparticles hybrids as substrates, owing to the stronger enhancement effect of AgNPs than AuNPs. Main vibrations of 6MP shown in the SERS spectrum were confirmed according to the reported work.<sup>33</sup> The band at 1000  $\text{cm}^{-1}$  is related to the Ag-S formation. The prominent feature of 6MP at 1280  $\text{cm}^{-1}$  is assigned to the C-N stretching. The other prominent peaks of 6MP at 613, 681, 859, 1141, 1326, 1386, 1473, 1585  $\text{cm}^{-1}$  was also observed in the SERS spectra. In addition, it was found that the SERS intensity of 6MP in the presence of GO/AgNPs was higher than that in the presence of MWCNT/AgNPs and SWCNT/AgNPs hybrids, so GO/AgNPs were chosen as SERS substrate for further 6MP detection.



**Fig. 5** The SERS spectra of 5  $\mu\text{mol L}^{-1}$  6MP on different substrates including GO/AuNPs (a), MWCNTs/AuNPs (b), SWCNTs/AuNPs (c); SWCNTs/AgNPs (d), MWCNTs/AgNPs (e), GO/AgNPs (f).

Choosing GO/AgNPs hybrids as substrates, SERS spectra of the 6MP with a series of concentrations are shown in Fig.6A. With the increasing concentrations of 6MP, the intensity of the SERS spectra increased regularly, which means the Raman intensity proportional to the number of 6MP molecules adsorbed on the GO/AgNPs. The SERS intensity of the vibration located at 1000  $\text{cm}^{-1}$  was plotted as a function of 6MP concentration in Fig.6B, which revealed a linear SERS response from 2  $\mu\text{mol L}^{-1}$  to 12  $\mu\text{mol L}^{-1}$  of 6MP ( $R^2=0.977$ ), the limit of detection (LOD) was calculated to be 1.05  $\mu\text{mol L}^{-1}$ . Considering that the as-prepared nanocomposites have high enhancement effect, it can be used as a potential SERS sensor to detect pharmaceutical drugs.

To assess the selectivity, some common potentially interfering substances including metal ions ( $\text{Na}^+$ ,  $\text{K}^+$ ,  $\text{Mg}^{2+}$ ), carbohydrate (glucose, lactose, sucrose), amino acids (lysine, histidine), purine analogue (ATP, GTP), were investigated to test the selectivity of this SERS system for 6MP detection. It was seen from Fig.7 that none of these substances caused obvious Raman signal alteration of SERS spectra of 6MP. Even though these substances were coexist with 6MP in solution, the SERS intensity of 6MP was changed weakly, which verified the good selectivity of this method. It should be noted that a little stronger SERS signal has been produced after adding 25  $\mu\text{mol L}^{-1}$  of L-histidine to the GO/AgNPs hybrids because it has its own SERS peak near 1000  $\text{cm}^{-1}$  which induced the intensity at 1000  $\text{cm}^{-1}$  has a little rise. While L-histidine coexistent with 6MP for SERS determination, no obvious alteration was observed contrast with individual 6MP. Namely, L-histidine has little effect on the Raman signal of 6MP, which might be owing to the stronger combination between 6MP with AgNPs than L-histidine.

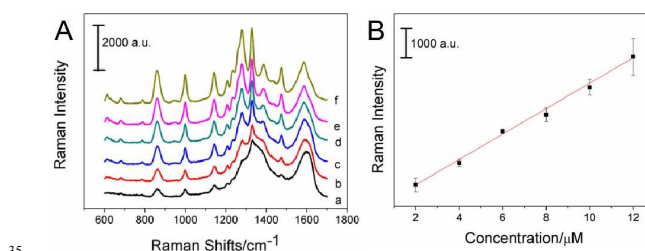


**Fig. 6** SERS spectra of different concentration of 6MP in water (A): 2  $\mu\text{mol L}^{-1}$  (a), 4  $\mu\text{mol L}^{-1}$  (b), 6  $\mu\text{mol L}^{-1}$  (c), 8  $\mu\text{mol L}^{-1}$  (d), 10  $\mu\text{mol L}^{-1}$  (e), 12  $\mu\text{mol L}^{-1}$  (f); and SERS dilution series of 6MP in water based on the peak located at 1000  $\text{cm}^{-1}$  (B).

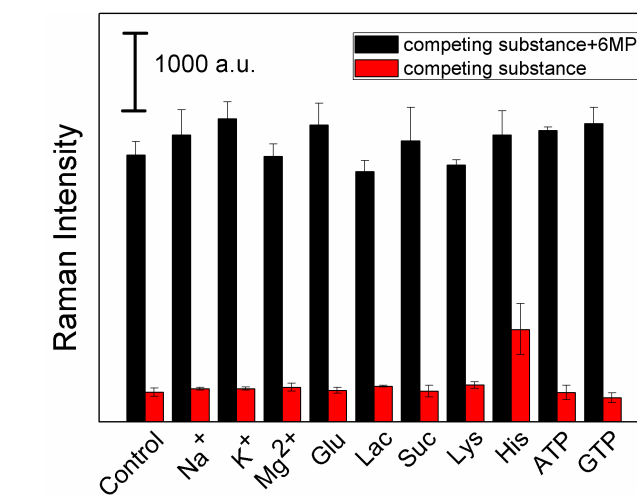


**Fig. 7** The selectivity of the proposed method. The concentration of 6MP is 6  $\mu\text{mol L}^{-1}$ . The addition of  $\text{Na}^+$ ,  $\text{K}^+$ , Glucose (Glu), Lactose (Lac), Sucrose (Suc), L-Lysine (Lys), L-Histidine (His) with the concentration of 25  $\mu\text{mol L}^{-1}$ . The concentration of  $\text{Mg}^{2+}$  is 10  $\mu\text{mol L}^{-1}$  and ATP, GTP is 8  $\mu\text{mol L}^{-1}$ .

**Table 1.** Results for the determination of 6MP in pharmaceutical tablets.

Normal	UV method	RSD n=3 (%)	SERS method	RSD n=3(%)
50mg	53.3mg	4.4	48.4mg	2.5

**Table 2.** Recovery of 6MP detection in pharmaceutical tablets.

Sample	Add( $\mu\text{mol L}^{-1}$ )	Found( $\mu\text{mol L}^{-1}$ )	Recovery(%)	RSD(n=3)
tablet	5.7	5.5 $\pm$ 0.2	92-99	3.5
	7.7	8.1 $\pm$ 0.9	92-114	10.8
	9.7	9.6 $\pm$ 0.3	96-101	3.5

Finally, determination of 6MP in pharmaceutical tablets was performed by this method. The determination in the tablet carried out by the SERS method was compared with standard UV-method. The experimental results in table 1 showed that there was no significant difference between the two methods. In order to evaluate whether or not the SERS method was valid in tablets detection, recovery studies of three concentrations with known amounts of 6MP were carried out on tablets samples. It was found that the recoveries of these samples are between 92% ~

114% (n=3) (Table 2). These results proved that the GO/AgNPs are appropriate SERS substrates for determination of 6MP in tablets.

#### 4. Conclusion

In conclusion, we have developed a new strategy to fabricate GO and MNPs hybrids with the use of PEI as linker molecule and the as-prepared hybrids have been successfully applied for 6MP detection. The assembly procedure is through the electrostatic assembly without any chemical modification and PEI linker is commercial without any organic synthesis step. Therefore, the assembly method is very simple. In addition, this method has been successfully applied for the assemblies of CNTs and MNPs. Thus it is general and can be applied for the construction of other nano-hybrids. Using the obtained GO/AgNPs nanocomposites as SERS substrates, a label free, sensitive and selective method to detect 6MP in pharmaceutical tablets has been demonstrated. This detection method can be easily applied for other targets detections, such as pharmaceutical, small biological molecules and environmental pollutants, by using their own special Raman scattering as detection signals.

#### Acknowledgment

This work was supported by the National Natural Science Foundation of China (NSFC, No. 21035005, 21305113), the fund of State Key Laboratory of Electroanalytical Chemistry (Changchun Institute of Applied Chemistry, Chinese Academy of Sciences) (SKLEAC201312), the fund of Chongqing Fundamental and Advanced Research Project (cstc2013jcyjA50008), the Fundamental Research Funds for the Central Universities (XDJK2012C057), the Research Fund for the Doctor Program of Southwest University (swu11077) and the special fund of Chongqing key laboratory (CSTC).

#### Notes and references

<sup>a</sup> Key Laboratory of Luminescent and Real-Time Analytical Chemistry (Southwest University), Ministry of Education, College of Chemistry and Chemical Engineering, Southwest University, 400715, Chongqing, P.R. China. Fax: 86-23-68367257; Tel: 86-23-68254059; E-mail: zsj@swu.edu.cn

<sup>b</sup> Key Laboratory of Luminescent and Real-Time Analytical Chemistry (Southwest University), Ministry of Education, College of Pharmaceutical Sciences, Southwest University, 400715, Chongqing, P.R. China. Fax: 86-23-68367257; Tel: 86-23-68254659; E-mail: chengzhi@swu.edu.cn

1. C.-C. Chang, K.-H. Yang, Y.-C. Liu, T.-C. Hsu and F.-D. Mai, *ACS Appl. Mater. Interfaces*, 2012, **4**, 4700-4707.
2. X. Ling, L. Xie, Y. Fang, H. Xu, H. Zhang, J. Kong, M. S. Dresselhaus, J. Zhang and Z. Liu, *Nano Lett*, 2010, **10**, 553-561.
3. Z. Liu, S. Tabakman, S. Sherlock, X. Li, Z. Chen, K. Jiang, S. Fan and H. Dai, *Nano Res*, 2010, **3**, 222-233.
4. K. Zimny, T. Roques-Carnes, C. Carteret, M. J. Stébé and J. L. Blin, *J. Phys. Chem. C*, 2012, **116**, 6585-6594.
5. W. Ren, Y. Fang and E. Wang, *ACS Nano*, 2011, **5**, 6425-6433.
6. M. Liu and W. Chen, *Biosens. Bioelectron.*, 2013, **46**, 68-73.
7. J. Huang, C. Zong, H. Shen, M. Liu, B. Chen, B. Ren and Z. Zhang, *Small*, 2012, **8**, 2577-2584.
8. X. Wang, C. Wang, L. Cheng, S.-T. Lee and Z. Liu, *J Am Chem Soc*, 2012, **134**, 7414-7422.
9. C. Hu, J. Rong, J. Cui, Y. Yang, L. Yang, Y. Wang and Y. Liu, *Carbon*, 2013, **51**, 255-264.
10. J. Liu, S. Fu, B. Yuan, Y. Li and Z. Deng, *J Am Chem Soc*,

- 2010, **132**, 7279-7281.
11. Y. Wang, S. J. Zhen, Y. Zhang, Y. F. Li and C. Z. Huang, *J Phys Chem C*, 2011, **115**, 12815-12821.
12. L. Zhang, S. J. Zhen, Y. Sang, J. Y. Li, Y. Wang, L. Zhan, L. Peng, J. Wang, Y. F. Li and C. Z. Huang, *Chem. Commun.*, 2010, **46**, 4303-4305.
13. F. A. He, J. T. Fan, F. Song, L. M. Zhang and H. L.-W. Chan, *Nanoscale*, 2011, **3**, 1182-1188.
14. X. Huang, X. Zhou, S. Wu, Y. Wei, X. Qi, J. Zhang, F. Boey and H. Zhang, *Small*, 2010, **6**, 513-516.
15. X. Zhou, Z. Chen, D. Yan and H. Lu, *J. Mater. Chem.*, 2012, **22**, 13506-13516.
16. J. Xiang and L. T. Drzal, *ACS Appl. Mater. Interfaces*, 2011, **3**, 1325-1332.
17. L. Feng, S. Zhang and Z. Liu, *Nanoscale*, 2011, **3**, 1252-1257.
18. X. Yang, G. Niu, X. Cao, Y. Wen, R. Xiang, H. Duan and Y. Chen, *J. Mater. Chem.*, 2012, **22**, 6649-6654.
19. E. Dillon, M. S. Bhutani and A. R. Barron, *J. Mater. Chem. B*, 2013, **1**, 1461-1465.
20. S.-J. Li, Y. F. Shi, L. Liu, L.-X. Song, H. Pang and J.-M. Du, *Electrochim. Acta*, 2012, **85**, 628-635.
21. E.-Z. Tan, P.-G. Yin, T.-T. You, H. Wang and L. Guo, *ACS Appl Mater Inter*, 2012, **4**, 3432-3437.
22. K. L. Nagashree, R. Lavanya, C. Kavitha, N. S. V. Narayanan and S. Sampath, *RSC Adv.*, 2013, **3**, 8356-8364.
23. X. Liu, L. Cao, W. Song, K. Ai and L. Lu, *ACS Appl Mater Inter*, 2011, **3**, 2944-2952.
24. R. Li, C. Han and Q.-W. Chen, *RSC Adv.*, 2013, **3**, 11715-11722.
25. W. L. Fu, S. J. Zhen and C. Z. Huang, *Analyst*, 2013, **138**, 3075-3081.
26. C. J. Orendorff, A. Gole, T. K. Sau and C. J. Murphy, *Anal. Chem.*, 2005, **77**, 3261-3266.
27. A. Kamińska, I. Dzieciulewski, J. L. Weyher, J. Waluk, S. Gawinkowski, V. Sashuk, M. Fiałkowski, M. Sawicka, T. Suski, S. Porowski and R. Hołyst, *J. Mater. Chem.*, 2011, **21**, 8662-8669.
28. F. Alvarez, C. A. Grillo, P. L. Schilardi, A. Rubert, G. Benitez, C. Lorente and M. F. L. d. Mele, *ACS Appl. Mater. Interfaces*, 2013, **5**, 249-255.
29. J. Du, Y. Wang and W. Zhang, *Chem. Eur. J.*, 2012, **18**, 8540-8546.
30. K. Ock, W. I. Jeon, E. O. Ganbold, M. Kim, J. Park, J. H. Seo, K. Cho, S.-W. Joo and S. Y. Lee, *Anal. Chem.*, 2012, **84**, 2172-2178.
31. J. Yang, Y. Cui, S. Zong, R. Zhang, C. Song and Z. Wang, *Mol. Pharmaceutics*, 2012, **9**, 842-849.
32. H. Chu, H. Yang, S. Huan, G. Shen and R. Yu, *J. Phys. Chem. B*, 2006, **110**, 5490-5497.
33. H. Yang, Y. Liu, Z. Liu, Y. Yang, J. Jiang, Z. Zhang, G. Shen, R. Yu, *J. Phys. Chem. B*, 2005, **109**, 2739-2744.